

How Active EMI Filter ICs Mitigate Common-Mode Emissions and Increase Power Density in Single- and Three-Phase Power Systems



Timothy Hegarty

ABSTRACT

A compact and efficient design of the electromagnetic interference (EMI) input filter is one of the main challenges in a high-density switching regulator, and is critical to achieving the full benefits of electrification in automotive, enterprise, aerospace and other highly constrained system environments. As examples, automotive on-board chargers and server-rack power supplies are high-power applications where it is important that the volumetric reduction of EMI filter components helps the solution fit into challenging form factors, especially with the advent of wide-bandgap (gallium nitride [GaN]- and silicon carbide [SiC]-based) power semiconductor devices with fast switching characteristics that potentially lead to higher common-mode (CM) emissions.

CM filters for both commercial (Class A) and residential (Class B) environments typically have limited Y-capacitance because of touch-current safety requirements, and thus require large-sized CM chokes to achieve the requisite attenuation – ultimately resulting in filter designs with bulky, heavy and expensive passive components. The deployment of active EMI filter (AEF) circuits enables more compact filter designs for next-generation power-conversion systems. Space-constrained applications, such as those mentioned above, are ripe for even further optimization by leveraging active power-supply-filter integrated circuits (ICs) to significantly reduce magnetic components and overall filter size.

This technical white paper frames the theoretical background and general principles of AEF circuits in terms of sensing, injection and control techniques, with practical circuit realizations using a family of stand-alone AEF ICs from Texas Instruments for CM noise cancellation in single-phase and three-phase AC power systems. Measured results from a 3.3-kW power factor correction (PFC) AC/DC regulator will illustrate the benefits of EMI mitigation and board space savings.

Table of Contents

1 Introduction	3
2 EMI Frequency Ranges	3
3 Passive EMI Filters for High-Power, Grid-Tied Applications	4
4 Active EMI Filters	5
5 Generalized AEF Circuits	6
6 Selection of the CM Active Filter Circuit	8
7 The Concept of Capacitive Amplification	9
8 Practical AEF Implementations	10
9 Practical Results	11
9.1 Low-Voltage Testing.....	11
9.2 High-Voltage Testing.....	12
10 Summary	14
11 References	15

List of Figures

Figure 2-1. Harmonic Current and Conducted EMI Frequency Ranges Classified by the IEC and CISPR.....	3
Figure 2-2. CISPR Quasi-Peak and Average Limits in the Frequency Range of 9 kHz to 30 MHz.....	3
Figure 3-1. Typical Two-Stage Passive EMI Filter for a Single-Phase System (a) and a Three-Phase System (b).....	4
Figure 3-2. Conventional Single-Phase Passive EMI Filter in a Totem-Pole PFC Reference Design.....	5
Figure 4-1. Fundamental Concept of AEF With Sensing, Gain and Injection Stages. The Control Structure can be FB (a) or FF (b).....	5
Figure 5-1. Basic Active Filter Structures in Their Single-Phase Equivalents – Four FB and Two FF Circuits – Categorized According to their Control, Sensing and Injection Techniques: FB-CSVI (a); FB-CSCI (b); FB-VSVI (c); FB-VSCI (d); FF-VSVI (e); and FF-CSCI (f).....	6
Figure 6-1. Simplified Schematic to Illustrate Basic Principles for CM Filtering and Injection Capacitor Multiplication.....	8
Figure 7-1. Example of Inject Branch Impedance Z_{INJ} With AEF Enabled vs. a Conventional Y-Capacitor, Showing the Boosted Equivalent Capacitance at Higher Frequencies by Active Feedback Action.....	9
Figure 8-1. Exemplary Single-Phase (a) and Three-Phase (b) AEF implementations for CM Attenuation.....	10
Figure 8-2. Internal Block Diagram of the TPSF12C3-Q1 Three-Phase Stand-Alone AEF IC.....	11
Figure 9-1. Schematic of Low-Voltage Test Setup.....	11
Figure 9-2. Single-Phase Filter Implementation With AEF.....	12
Figure 9-3. EN 55032 Class B EMI Results With AEF Disabled and Enabled.....	12
Figure 9-4. EMI Performance With TIDM-1007: AEF Disabled vs. Enabled Using the Same Filter.....	13
Figure 9-5. EMI Performance with TIDM-1007: A Small-Choke AEF Design Compared to a Large-Choke Passive Filter.....	13
Figure 9-6. Size Reduction Enabled by AEF: Passive Filter (a); Active Filter (b).....	13
Figure 9-7. Area, Volume, Cost and Weight Reduction Enabled by AEF (a); Choke Size Comparison (b).....	13
Figure 9-8. Impedance Characteristics of the Selected CM Chokes in the Passive Design (2×12 mH) and Active Design (4 mH and 1 mH).....	14

List of Tables

Table 5-1. AEF Circuits From Figure 5-1 Categorized by Topology (Control, Sensing and Injection Techniques).....	7
Table 9-1. CM Choke Component Details for the Passive and Active Filter Implementations.....	14

Trademarks

All trademarks are the property of their respective owners.

1 Introduction

Common-mode (CM) EMI filters for high-density applications often have a limit to the total value of Y-capacitance – related to touch-current safety requirements – and thus require large-sized CM chokes to achieve a target corner frequency or filter attenuation characteristic. The result is a compromised passive filter design with bulky, heavy and expensive CM chokes that dominate the overall filter size.

However, active EMI filter (AEF) circuits enable more compact filter designs for next-generation power management systems. As such, space-constrained applications can use [active power-supply filter integrated circuits](#) (ICs) to reduce magnetic component and overall filter size. Ancillary benefits include lower power losses for better thermal management and higher reliability, easier mechanical and packaging designs, reduced electromagnetic coupling among components within a confined space, and lower cost.

2 EMI Frequency Ranges

High-frequency switching networks are essential components for energy conversion in switched-mode AC/DC regulators. Yet these switching networks are also inherent sources of input current harmonics and conducted EMI that can affect the normal operation of adjacent equipment sharing the same grid-connected input source.

Figure 2-1 depicts the harmonic and conducted EMI frequency ranges classified by electromagnetic compatibility (EMC) standards organizations, such as the International Electrotechnical Commission (IEC) and Comité International Spécial des Perturbations Radioélectriques (CISPR).

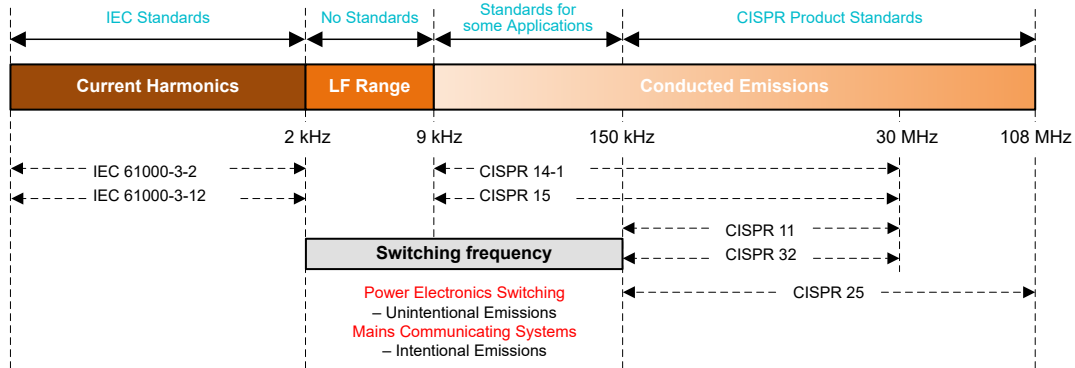


Figure 2-1. Harmonic Current and Conducted EMI Frequency Ranges Classified by the IEC and CISPR

Applying PFC techniques enables input current harmonics to meet limits set by IEC 61000-3-2/-12 at frequencies up to 2 kHz. EMI filters are still mandatory, however, in order to attenuate high-frequency noise currents and meet conducted emissions specifications (such as CISPR 11 for industrial and CISPR 25 for automotive applications) within classified frequency ranges beginning at 150 kHz [1], as illustrated in Figure 2-2.

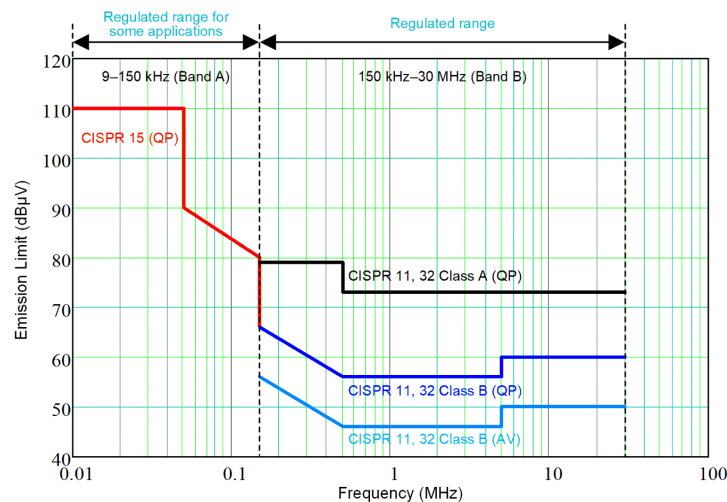


Figure 2-2. CISPR Quasi-Peak and Average Limits in the Frequency Range of 9 kHz to 30 MHz

As Figure 2-2 indicates, only the CISPR 14-1 and CISPR 15 product standards – for household appliances and lighting applications, respectively – presently specify emissions limits as low as 9 kHz. However, with standardization activities ongoing, the forthcoming inclusion of the 9- to 150-kHz band and applicable emissions limits to the existing IEC 61000-6-3 generic EMI standard [1-2] will surely affect the future design of EMI filters for attenuation below 150 kHz. EMI mitigation across wide frequency ranges require correspondingly larger passive components.

3 Passive EMI Filters for High-Power, Grid-Tied Applications

Complying with EMC regulations intended to limit the levels of conducted emissions requires the insertion of a low-pass EMI filter between a switching regulator and the mains input source. Figure 3-1 illustrates typical filter arrangements for single-phase (three-wire) and three-phase (four-wire) systems in kilowatt-scale, grid-connected applications. L, N and PE refer to live, neutral and protective earth terminals, respectively. Multistage filters as shown provide high rolloff and are common in high-power AC line applications where CM noise is often more challenging to mitigate than differential-mode (DM) noise. Although Figure 3-1 omits components for surge pulse protection and resistive discharge, the schematic does incorporate a line impedance stabilization network (LISN) in series with the input supply to enable measurement of the total EMI, including DM and CM propagation components.

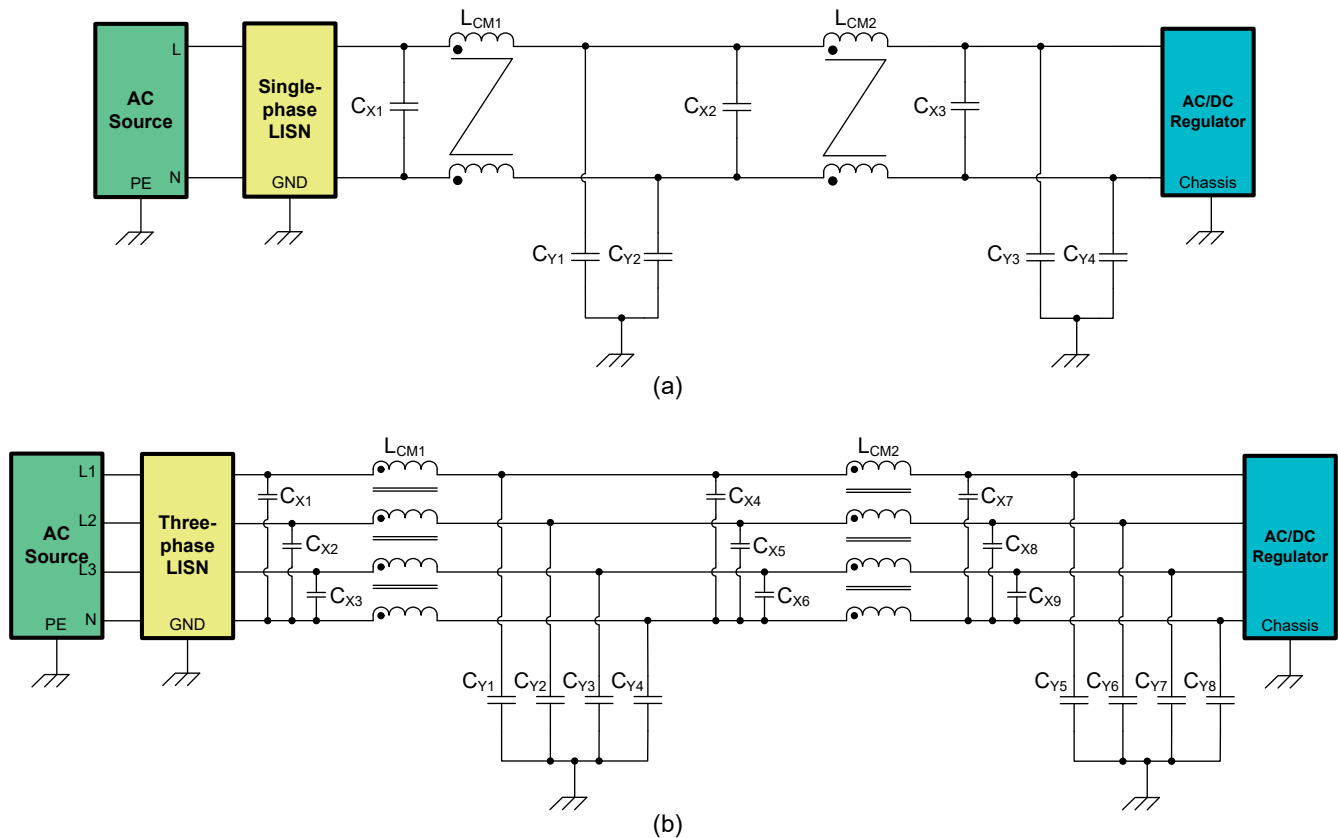


Figure 3-1. Typical Two-Stage Passive EMI Filter for a Single-Phase System (a) and a Three-Phase System (b)

At a higher level, passive EMI filters represent an intuitive, straightforward and traditional approach to mitigate the conducted emissions of a power electronic circuit, even though the size, weight and cost of the passive components cause significant constraints in some applications. Such passive filter designs rely on the insertion of high-impedance series elements (DM inductors, CM chokes) and low-impedance shunt elements (X- and Y-capacitors) to create an impedance mismatch in the EMI current propagation path. The low-order switching harmonics usually dictate the size of the reactive filter components based on the required corner frequency (or multiple corner frequencies in multistage designs).

Taking the single-phase schematic in [Figure 3-1](#) as an example, CM chokes L_{CM1} and L_{CM2} and Y-rated capacitors C_{Y1} to C_{Y4} (connected between the AC power lines and earth ground) provide CM attenuation. The CM current sourced from the switching regulator returns first through the regulator-side Y-capacitors and next through the Y-capacitors positioned between the CM chokes. The alternative return path of any remaining CM current is through the measuring impedance of the LISN setup – obviously to the detriment of EMI performance.

As mentioned in the introduction, safety regulations limit the total Y-capacitance to relatively low values (often under 10 nF), and the CM inductance of the chokes required for a desired corner frequency is relatively high, in the range of several millihenries – making the chokes large, heavy and expensive. In contrast for DM attenuation, the X-capacitors C_{X1} to C_{X3} can be large-valued (typically 2.2 μ F), allowing low-valued DM inductances using the leakage inductance of the CM chokes.

In effect, CM chokes dominate the size of the EMI filter, as illustrated by the practical implementation [3] shown in [Figure 3-2](#), and bring several challenges during EMI filter design – including bulky volume, thermal management issues, acoustic noise, filter resonances and electromagnetic coupling between components. In addition, parasitic elements of the filter components (especially CM chokes) affect high-frequency performance and achievable attenuation. The discrete components used in the filter come in different form factors from various manufacturers and are not optimized to fit well with each other, compromising the spatial design and assembly of the filter implementation.

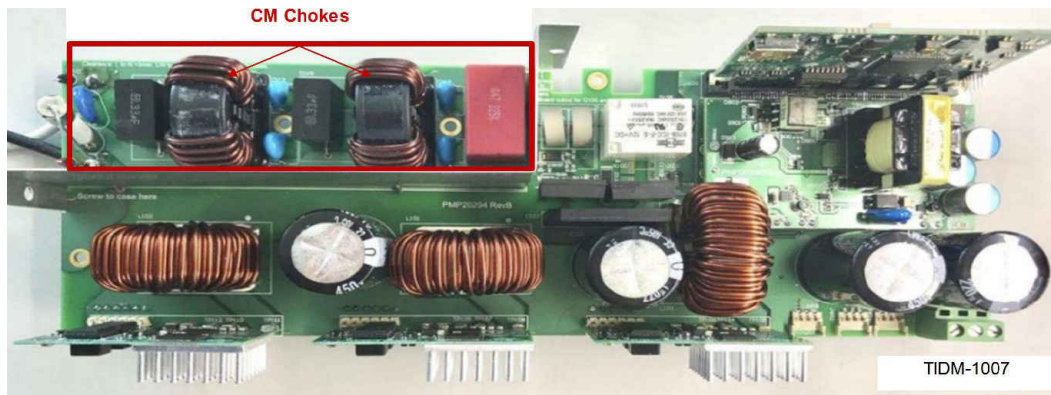


Figure 3-2. Conventional Single-Phase Passive EMI Filter in a Totem-Pole PFC Reference Design

4 Active EMI Filters

There have been numerous publications [4-7] detailing the application of AEF, with results yielding a substantial reduction in filter size and volume relative to a conventional passive-only design. Much like a passive EMI filter, the AEF circuit connects to the lines between the EMI source and the EMI victim, as shown in [Figure 4-1](#).

Unlike a passive filter, however, an AEF circuit uses active devices and control to sense the residual (DM or CM) voltage or current disturbance, and injects an opposing signal that directly negates that noise disturbance. Based on the superposition theorem of signals with equal amplitude and opposite phase, the injected voltage or current can theoretically cancel or nullify the incident noise voltage or current contribution from the EMI source – essentially a destructive interference. This strategy is commonly applied in acoustics and successively for EMI.



Figure 4-1. Fundamental Concept of AEF With Sensing, Gain and Injection Stages. The Control Structure can be FB (a) or FF (b)

The expectation is that AEF significantly reduces EMI, resulting in a smaller-size filter versus a traditional passive-only design with equivalent attenuation. Along with AEF, other (smaller) passive components interface to the power stage and improve the overall attenuation – these circuits are known as hybrid EMI filters (HEFs). The design and implementation of AEF and HEF circuits depend on the path of conduction (DM or CM) and the required sensing, gain and injection stages. As shown in Figure 4-1, the cancellation signal is directly generated from a measured signal by a feedback (FB) or feedforward (FF) approach.

5 Generalized AEF Circuits

Figure 5-1 illustrates six active-filter configurations generalized according to the sensed noise parameter (voltage or current), the means by which the cancellation signal is injected (voltage or current), and the active control technique (FB or FF).

- Voltage sense (VS) or current sense (CS)
- Voltage injection (VI) or current injection (CI)
- FB control or an FF control structure

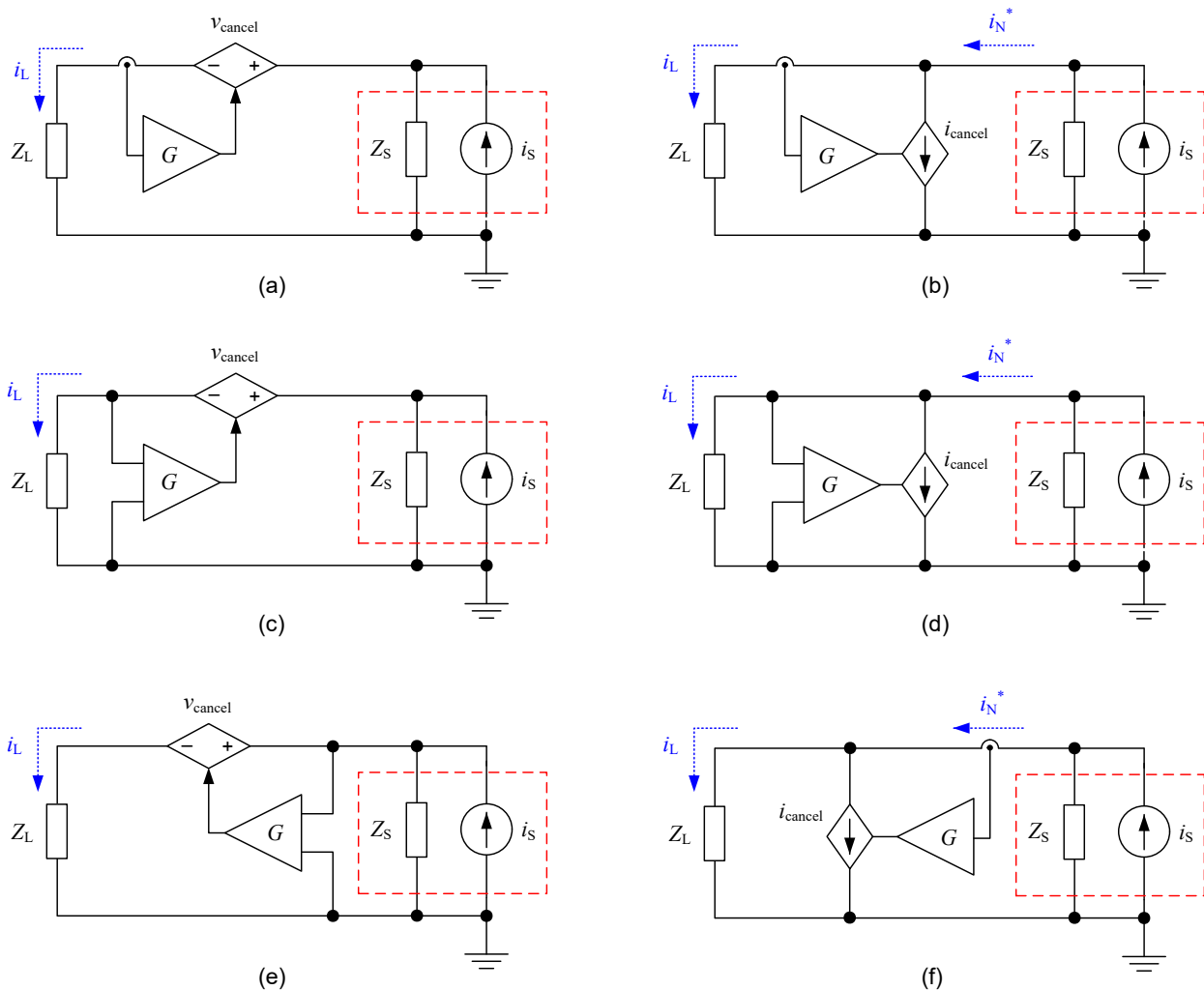


Figure 5-1. Basic Active Filter Structures in Their Single-Phase Equivalents – Four FB and Two FF Circuits – Categorized According to their Control, Sensing and Injection Techniques: FB-CSVI (a); FB-CSCI (b); FB-VSVI (c); FB-VSCI (d); FF-VSVI (e); and FF-CSCI (f)

The terms i_S and Z_S in Figure 5-1 designate the Norton-equivalent noise current source and parallel source impedance of the power stage. Z_L is the load impedance at the noise-receiving end (or the EMI victim); for example, the LISN for EMI measurement. G represents the gain of the active circuit. Adding different passive elements in place of Z_S and Z_L will form different hybrid circuits.

From a control standpoint, FB designs sense the residual disturbance at the EMI victim, invert the signal, amplify it with a high gain G , and inject a cancellation signal back into the system to drive the sensed parameter to zero over the required frequency range. In contrast, FF designs sense the disturbance at the EMI source, invert the signal, amplify it with unity gain and inject it back at the EMI victim. The amplifier unity-gain setting for FF must be highly accurate such that the EMI and anti-EMI signals cancel, making FF designs more difficult to design.

In terms of noise sensing, the VS and CS elements are typically capacitors and CS transformers (or auxiliary windings on existing magnetics), respectively. In terms of noise cancellation, VI designs use a controlled series voltage source to impede the flow of noise current to the LISN, whereas CI designs involve a controlled shunt current source to reroute the flow of the noise current produced by the noise source to prevent it from flowing in and being measured by the LISN. VI and CI designs effectively create a voltage divider and current divider, respectively, with the load. In general, transformers can embody the series element, whereas capacitors implement a shunt conduction path.

Table 5-1 summarizes the salient characteristics of the AEF circuits embodied in Figure 5-1, including expressions for insertion loss and circuit conditions for high attenuation [4]. Y_S and Y_L represent the admittance of the noise source and load, respectively, for a FB-VSCI design.

Table 5-1. AEF Circuits From Figure 5-1 Categorized by Topology (Control, Sensing and Injection Techniques)

AEF Topology		Control (FB/FF)	Sensing (VS/CS)	Injection (VI/CI)	Insertion Loss (IL)	High-Attenuation Condition
a	FB-CSVI	Feedback	Current	Voltage	$\left 1 + \frac{G}{Z_S + Z_L} \right $	$ G \gg Z_S + Z_L $
b	FB-CSCI	Feedback	Current	Current	$\left 1 + \frac{Z_S}{Z_S + Z_L} \cdot G \right $	$ Z_S \gg Z_L $
c	FB-VSVI	Feedback	Voltage	Voltage	$\left 1 + \frac{Z_L}{Z_S + Z_L} \cdot G \right $	$ Z_S \ll Z_L $
d	FB-VSCI	Feedback	Voltage	Current	$\left 1 + \frac{G}{Y_S + Y_L} \right $	$ G \gg Y_S + Y_L $
e	FF-VSVI	Feedforward	Voltage	Voltage	$\left \frac{1}{1-G} \cdot \left(1 - \frac{Z_S}{Z_S + Z_L} \cdot G \right) \right $	$G = 1, Z_S \ll Z_L $
f	FF-CSCI	Feedforward	Current	Current	$\left \frac{1}{1-G} \cdot \left(1 - \frac{Z_L}{Z_S + Z_L} \cdot G \right) \right $	$G = 1, Z_S \gg Z_L $

$IL = i_{L,w/oAEF} / i_{L,w/AEF}$ is the quotient of the filter output current without and with AEF installed, normally measured with 50- Ω source and load impedances, and correlates to the achievable attenuation of EMI. As indicated in Table 5-1, each AEF topology requires a specific impedance behavior to achieve high attenuation.

6 Selection of the CM Active Filter Circuit

Since magnetic components for both CS and VI are large-sized and likely custom parts (offsetting the size reduction enabled by AEF), it's a good idea to select an AEF topology that precludes the use of additional magnetic components. The VSCI implementation leverages capacitors in combination with low-voltage active circuits for sensing and injection, and thus achieves a smaller size [5].

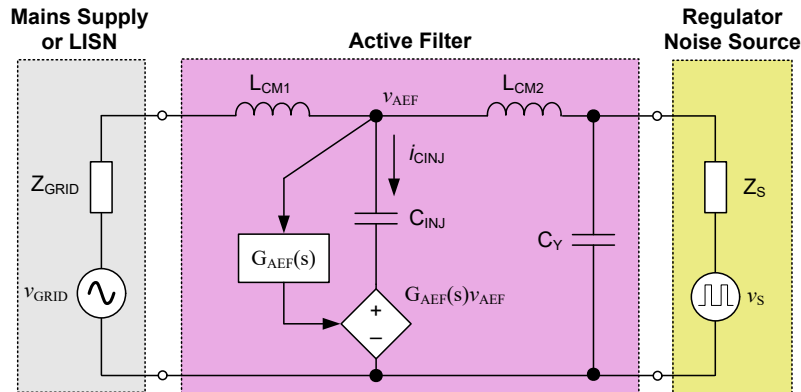


Figure 6-1. Simplified Schematic to Illustrate Basic Principles for CM Filtering and Injection Capacitor Multiplication

Figure 6-1 shows a simplified single-phase schematic to illustrate the basic principle of the selected FB-VSCI circuit in a CM filter setup. As mentioned previously, the main idea with this AEF topology is to use an injection capacitor with a value similar to the Y-capacitance in an equivalent passive filter in order to reduce the values of the CM chokes, which are the largest components in high-power filters.

The Thevenin-equivalent CM noise source consists of voltage source v_S in series with source impedance Z_S , which is considered capacitive. The mains impedance Z_{GRID} is typically inductive. CM chokes, designated as L_{CM1} and L_{CM2} , also function as decoupling elements to achieve high source and load impedances, as required for a high-attenuation FB-VSCI design (see row "d" in Table 5-1).

With Y-rated sense and injection capacitors connected to the AC lines, the purpose of the circuit is to reduce the total filter volume, yet maintain low values of the low-frequency earth leakage current using an active circuit that shapes the frequency response of the injection capacitor – effectively increasing its value for high frequencies. In turn, this amplified injection capacitance over the frequency range of interest is the key to lower CM choke inductances relative to values of a passive filter with equivalent attenuation.

The circuit advantages are:

- A simple filter structure with a wide operating frequency range and high stability margins.
- A reduced CM choke size for lower volume, weight, power loss and cost, while also resulting in better high-frequency performance given lower choke self-parasitics and a higher self-resonant frequency (f_{SRF}).
- No additional magnetic components – only Y-rated sense and injection capacitors, with minimal impact to peak touch current (measured according to IEC 60990).
- Enhanced safety using a low-voltage AEF IC referenced to chassis ground.
- A stand-alone AEF IC that provides flexibility in terms of placement near the filter components.
- Surge immunity to line voltage surges to help meet IEC 61000-4-5.

7 The Concept of Capacitive Amplification

An AEF circuit for CM noise mitigation either amplifies the apparent inductance of a CM choke or the apparent capacitance of a Y-capacitor over the frequency range of interest. A VSCI AEF configured for CM attenuation uses an amplifier stage as a capacitive multiplier of the injection capacitor, C_{INJ} . It is this higher value of active capacitance that supports lower values for the CM chokes to achieve a target attenuation.

Looking at [Figure 6-1](#), [Equation 1](#) shows that the injection capacitance is effectively multiplied by G_{AEF} , the CM voltage gain from the power lines to the amplifier output:

$$v_{C_{INJ}} = [1 - G_{AEF}(f)]v_{AEF} \tag{1}$$

$$i_{C_{INJ}} = C_{INJ} \frac{dv_{C_{INJ}}}{dt} = [1 - G_{AEF}(f)] C_{INJ} \frac{dv_{AEF}}{dt}$$

$$\Rightarrow C_{INJ,active}(f) = |1 - G_{AEF}(f)| C_{INJ}$$

[Figure 7-1](#) shows a simulated plot of an injection network impedance when a FB-VSCI AEF circuit is enabled and disabled. The lower impedance above 2 kHz (and especially above 100 kHz) is caused by the capacitive amplification by the active circuit of a 4.7-nF injection capacitor and its associated damping network.

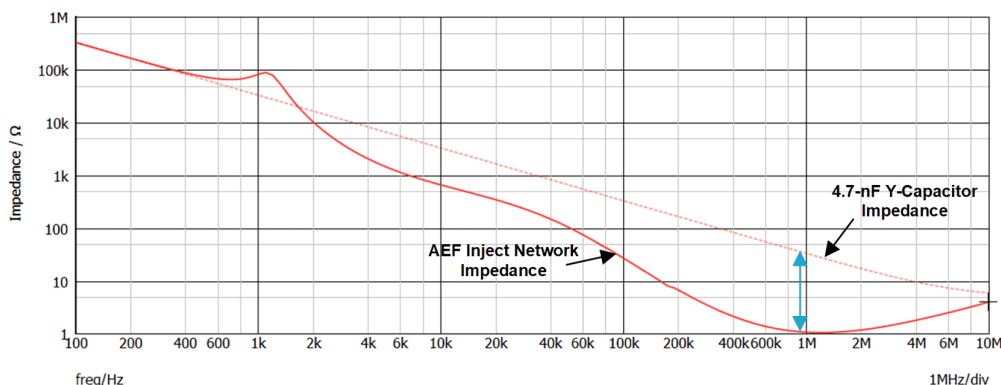


Figure 7-1. Example of Inject Branch Impedance Z_{INJ} With AEF Enabled vs. a Conventional Y-Capacitor, Showing the Boosted Equivalent Capacitance at Higher Frequencies by Active Feedback Action

8 Practical AEF Implementations

Figure 8-1 shows practical AEF implementations for CM attenuation with a FB-VSCI configuration using the TPSF12C1, TPSF12C1-Q1, TPSF12C3 and TPSF12C3-Q1 stand-alone AEF IC family in single- and three-phase power systems [8-11]. The setups are similar to the two-stage passive filters in Figure 3-1, except that the AEF IC is now positioned between the CM chokes to provide a lower-impedance shunt path for CM currents.

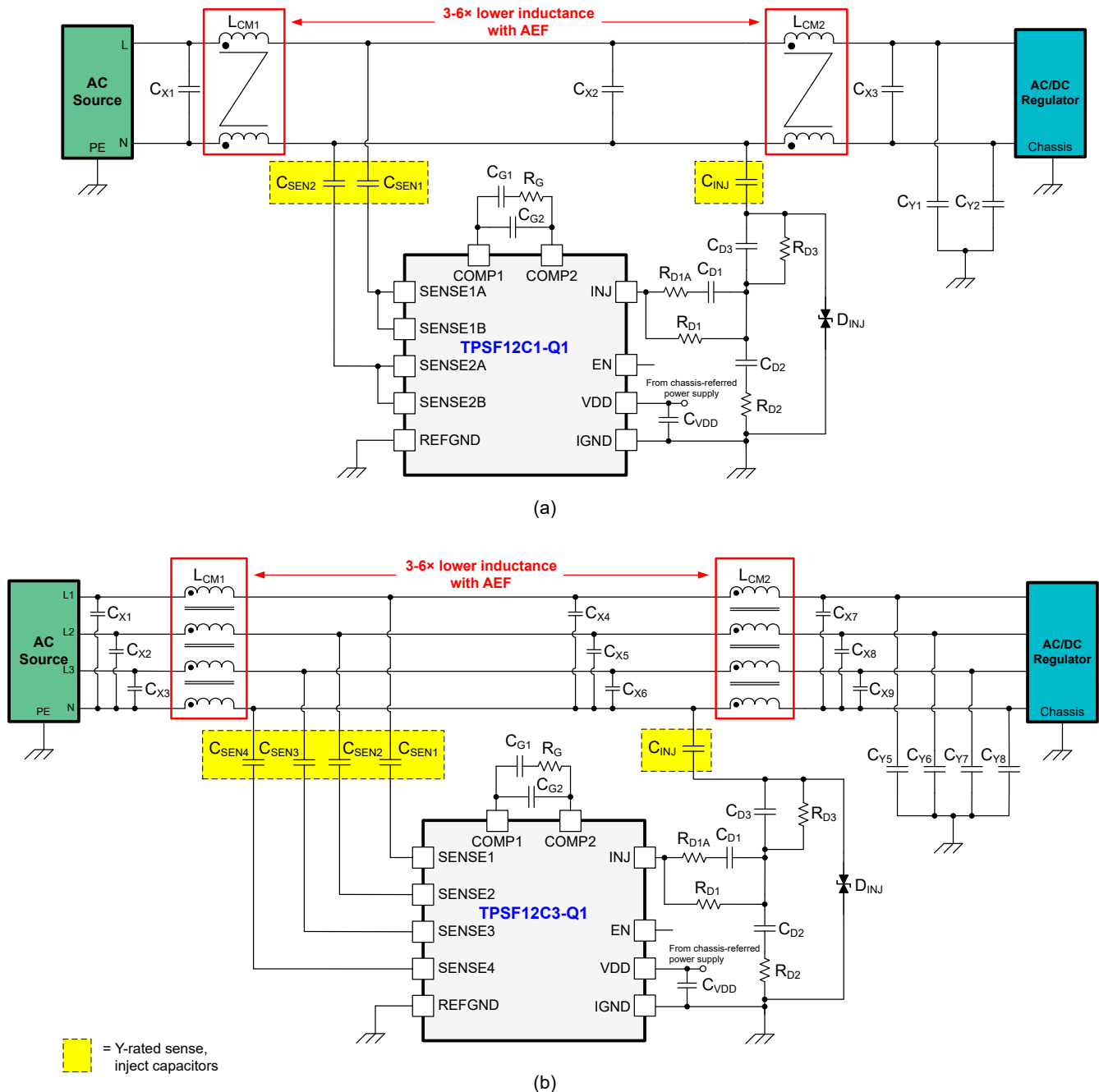


Figure 8-1. Exemplary Single-Phase (a) and Three-Phase (b) AEF implementations for CM Attenuation

The sense pins of this device family interface with the power lines using a set of Y-rated sense capacitors, typically 680 pF, and feed into a high-pass filter and signal combiner, as shown in the IC block diagram of Figure 8-2. The IC rejects both the line-frequency (50- or 60-Hz) AC voltage as well as DM disturbances, while amplifying high-frequency CM disturbances and maintaining closed-loop stability using an external tunable damping circuit.

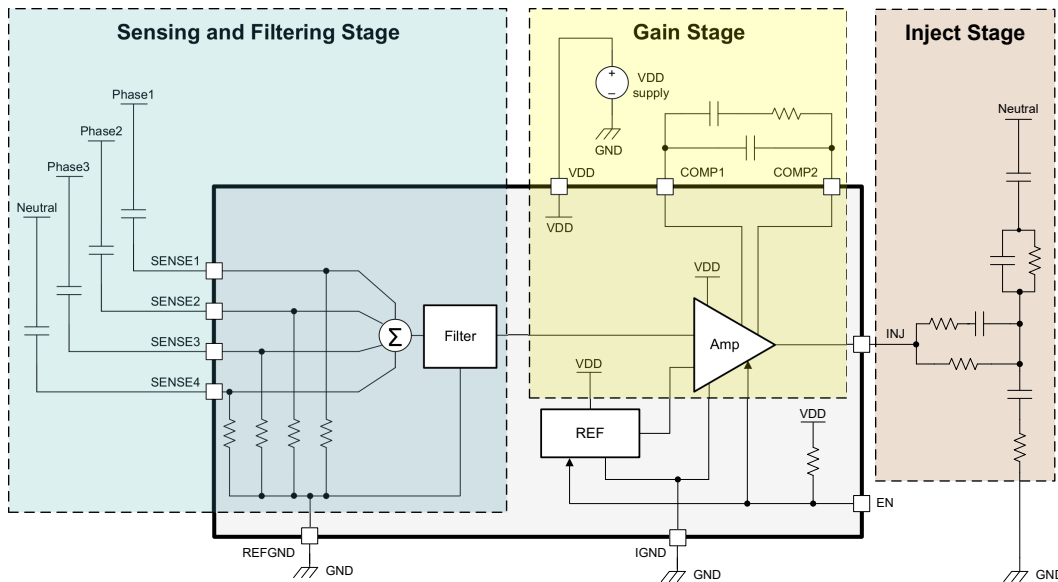


Figure 8-2. Internal Block Diagram of the TPSF12C3-Q1 Three-Phase Stand-Alone AEF IC

The components between the COMP1 and COMP2 pins form a lead-lag network that sets the amplification gain characteristic. The output of the power amplifier at INJ injects the required noise-canceling signal back into the power lines through a damping and stability network (see components with subscript “D” reference designators in Figure 8-1), and a Y-rated injection capacitor C_{INJ} , typically 4.7 nF. The IC includes integrated filtering, compensation and protection circuitry. The VDD bias supply ranges from 8 V to 16 V, nominally 12 V, and references to system chassis ground.

The X-capacitor(s) placed between the two CM chokes effectively provide a low-impedance path between the power lines from a CM standpoint, typically up to low-megahertz frequencies. This path allows current injection onto one power line, typically neutral, using only one injection capacitor. If the three-phase filter is a three-wire system without a neutral wire, the SENSE4 pin of the TPSF12C3-Q1 ties to ground and the injection capacitor couples through an artificial star-point connection of the X-capacitors.

9 Practical Results

9.1 Low-Voltage Testing

Figure 9-1 shows the schematic of a single-phase AEF circuit with CM noise attenuation achieved using the TPSF12C1-Q1 active filter IC. The design includes both regulator-side and grid-side Y-capacitors. A LISN provides a suitable interface to an EMI receiver for EMI measurement from 150 kHz to 30 MHz.

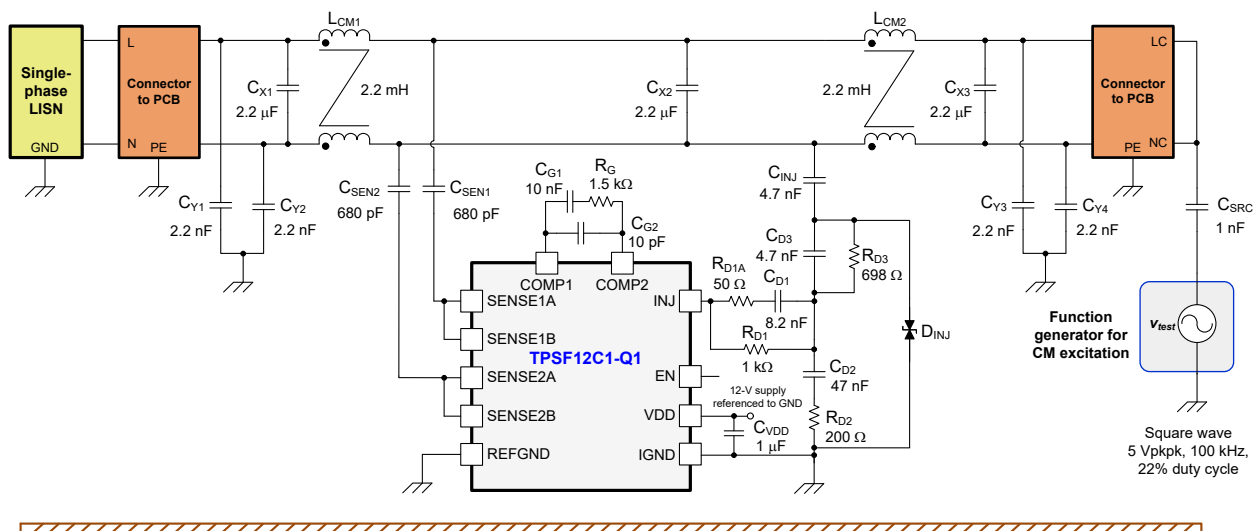


Figure 9-1. Schematic of Low-Voltage Test Setup

As shown in [Figure 9-1](#), a square-wave signal derived from a function generator represents a convenient source for CM noise excitation, and a 1-nF capacitor mimics a realistic CM noise-source impedance of a switching regulator. Adjusting the amplitude and transition times of the source voltage sets a suitable noise amplitude and spectral envelope measured at the LISN.

This simple low-voltage test with signal injection facilitates a safe and expedient performance characterization of the filter in an EMI chamber prior to connection to a switching regulator in a high-voltage operating environment.

[Figure 9-2](#) shows the filter board implementation. [Figure 9-3](#) presents EMI results with AEF disabled and enabled, using both quasi-peak (QP) and average (AV) noise detectors. As evident in [Figure 9-3](#), AEF provides up to 30 dB of CM noise attenuation in the low-frequency range (100 kHz to 3 MHz), which allows a filter using two 2-mH nanocrystalline chokes to achieve an equivalent CM attenuation performance as a passive filter design with two 12-mH chokes.

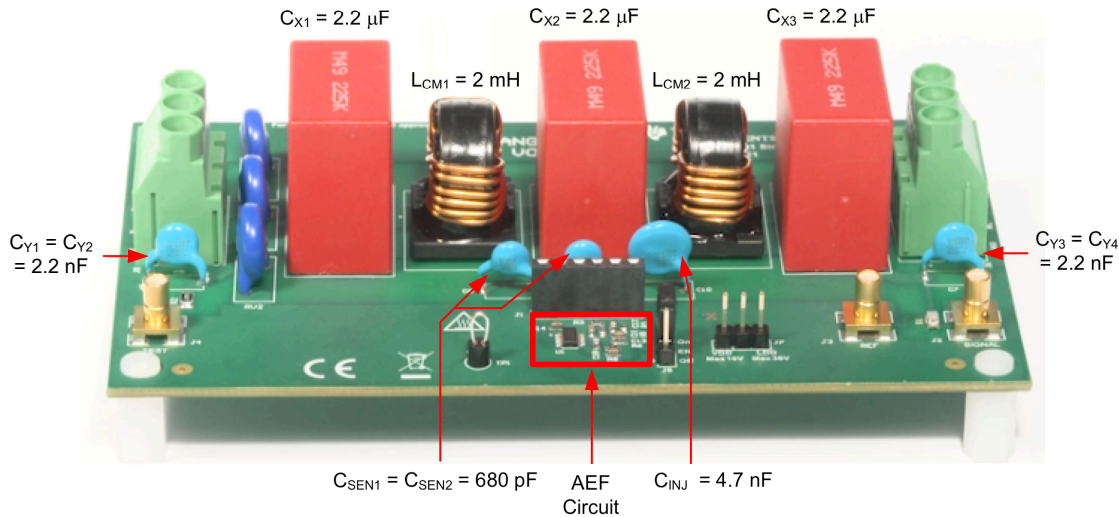
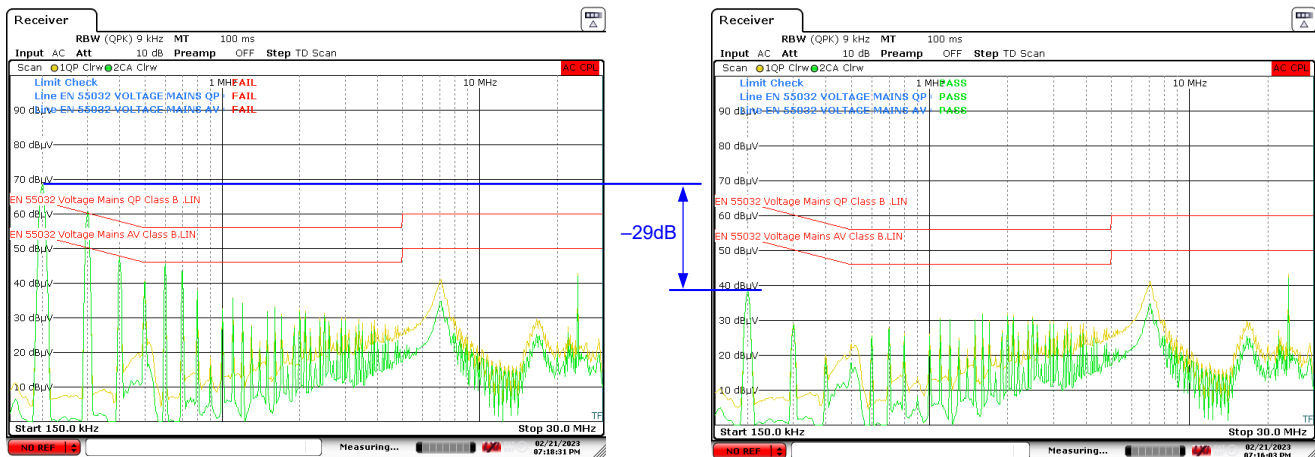


Figure 9-2. Single-Phase Filter Implementation With AEF



AEF disabled

(a)

AEF enabled

(b)

Figure 9-3. EN 55032 Class B EMI Results With AEF Disabled and Enabled

9.2 High-Voltage Testing

[Figure 9-4](#) and [Figure 9-5](#) show the measured CM EMI performance with the TPSF12C1-Q1 single-phase AEF IC using the power stage of the [High-Efficiency GaN CCM Totem-Pole Bridgeless Power Factor Correction \(PFC\) Reference Design](#) (TIDM-1007 shown in [Figure 3-2](#)), which is a 3.3-kW single-phase bridgeless PFC converter [3] with LMG3410 GaN power devices switching at 100 kHz.

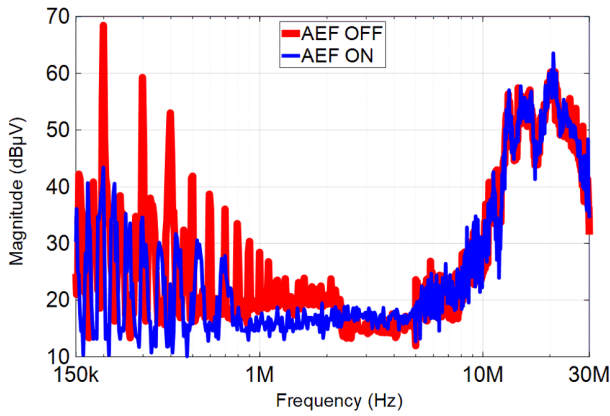


Figure 9-4. EMI Performance With TIDM-1007: AEF Disabled vs. Enabled Using the Same Filter

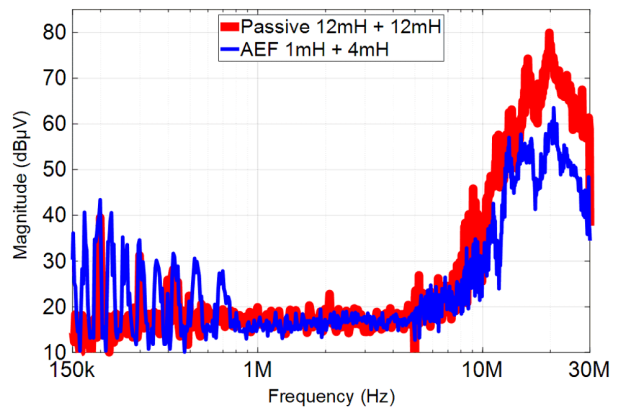


Figure 9-5. EMI Performance with TIDM-1007: A Small-Choke AEF Design Compared to a Large-Choke Passive Filter

As evident in [Figure 9-4](#), the AEF provides 15 to 30 dB of CM noise attenuation in the low-frequency range (150 kHz to 3 MHz), which enables a filter using 1- and 4-mH nanocrystalline chokes to achieve an equivalent CM attenuation performance as a passive filter design with two 12-mH chokes, as shown in [Figure 9-5](#). To support a fair comparison, these chokes derive from the same component family with a similar core material (vendor: Würth Elektronik). In addition, the smaller-size chokes of the AEF-based design provide better attenuation at frequencies above 10 MHz given the lower intrawinding parasitic capacitance.

[Figure 9-6](#) shows photos of the filters used for the EMI results presented in [Figure 9-5](#). The AEF enables a 52% reduction in box volume of the CM chokes, as highlighted in [Figure 9-7](#).

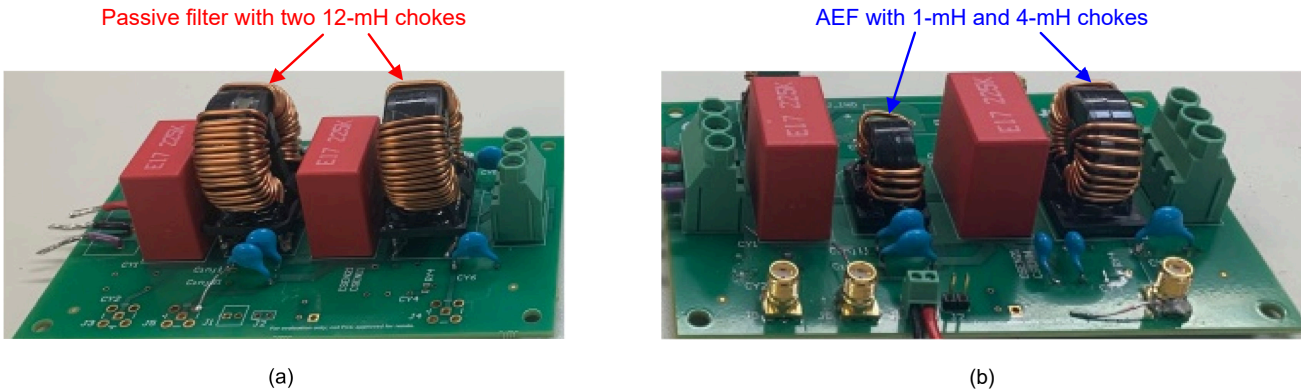


Figure 9-6. Size Reduction Enabled by AEF: Passive Filter (a); Active Filter (b)

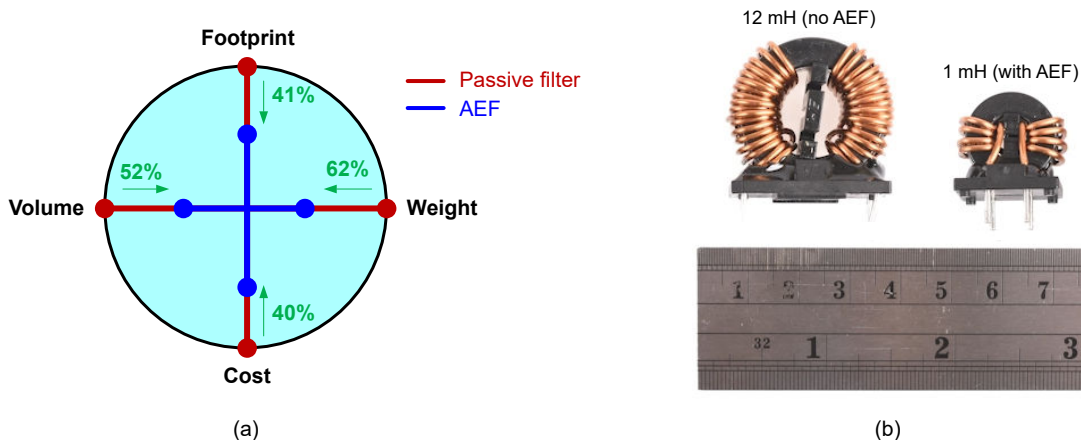


Figure 9-7. Area, Volume, Cost and Weight Reduction Enabled by AEF (a); Choke Size Comparison (b)

Table 9-1 captures the applicable parameters for the CM chokes highlighted in Figure 9-6. The AEF achieves a 60% total copper loss reduction at 10 A_{RMS} ($P_{Cu} = 6\text{ W} - 2.36\text{ W} = 3.64\text{ W}$, neglecting the winding resistance increase from temperature rise), which implies lower component operating temperatures and improved capacitor lifetimes.

Table 9-1. CM Choke Component Details for the Passive and Active Filter Implementations

Filter	CM Choke Part Number	Quantity	L _{CM} (mH)	R _{DCR} (mΩ)	f _{SRF} (MHz)	Size (L × W × H, mm)	Mass (g)	P _{Cu} (W)
Passive	7448051012	2	12	15	0.8	23 × 34 × 33	36	3.0
Active	7448041104	1	4	8.5	10	19 × 28 × 28	17	1.7
	7448031501	1	1	3.3	40	17 × 23 × 25	10	0.66

Figure 9-8 provides impedance curves for the CM chokes to highlight the smaller-size components that have a higher self-resonant frequency and improved high-frequency performance. As an example of the higher CM impedance at high frequencies because of the lower intrawinding capacitance, the impedance of the grid-side CM choke at 30 MHz increases from 150 Ω to 1.1 kΩ (when going from 12 mH in the passive design to 1 mH in the active design). The × and o markers shown at 10 MHz and 30 MHz in Figure 9-8 demarcate the respective impedances for passive and active designs. The higher choke impedance above 10 MHz for active designs largely obviates the need for grid-side Y-capacitors.

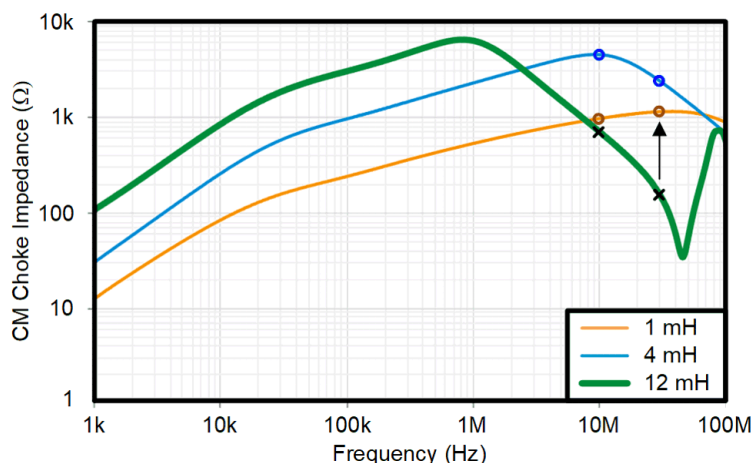


Figure 9-8. Impedance Characteristics of the Selected CM Chokes in the Passive Design (2 × 12 mH) and Active Design (4 mH and 1 mH)

As expected, horizontally mounted chokes in three-phase circuits can generally yield even larger percentage footprint reductions relative to the vertically mounted chokes common in single-phase designs.

10 Summary

Recent developments in power semiconductor technology and packaging enable power-supply implementations with increased efficiency and power density. However, the improved switching performance and smaller packaging that makes these gains possible is also in part responsible for elevating CM emission signatures. The shift of next-generation power electronics toward higher densities, improved performance, reduced weight and lower cost necessitates a new approach to EMI filter design. Within this context, a compact and efficient design for the EMI filter stage is one of the key challenges in high-density switching regulator designs, particularly for automotive and industrial applications where solution size and cost are important considerations.

Practical results from an active filter implementation (detailed above) to suppress the measured CM noise signature indicate a significant volumetric reduction of the CM choke components when benchmarked against an equivalent passive-only design. Additional benefits include reduced power loss for better thermal management and increased system-level reliability, lower component weight for better mechanical robustness, improved high-frequency performance due to lower choke parasitic capacitance, and reduced costs.

11 References

1. Texas Instruments white paper: [An Overview of Conducted EMI Specifications for Power Supplies](#)
2. Texas Instruments white paper: [An Engineer's Guide to Low EMI in DC/DC Regulators](#)
3. "High Efficiency GaN CCM Totem Pole Bridgeless Power Factor Correction (PFC) Reference Design." Texas Instruments reference design No. TIDM-1007.
4. Son, Yo-Chan, and Sul, Seung-Ki. "Generalization of Active Filters for EMI Reduction and Harmonics Compensation." Published in *IEEE Transactions on Industry Applications*, vol. 42, no. 2 (March-April 2006): pp. 545-551.
5. Heldwein, Marcelo Lobo, Hans Ertl, Juergen Biela, and Johann W. Kolar. "Implementation of a Transformerless Common-Mode Active Filter for Offline Converter Systems." Published in *IEEE Transactions on Industrial Electronics*, vol. 57, no. 5 (May 2010): pp. 1772-1786.
6. Narayanasamy, Balaji, and Luo, Fang. "A Survey of Active EMI Filters for Conducted EMI Noise Reduction in Power Electronic Converters." Published in *IEEE Transactions on Electromagnetic Compatibility*, vol. 61, no. 6 (December 2019): pp. 2040-2049.
7. Kumar, Ashish, Hou, Yuetao, Ramadass, Yogesh, Merkin, Tim, Hegarty, Timothy, Obidat, Abdallah. "An Active EMI filter for High-Power Off-Line Applications." Published in *2023 Applied Power Electronics Conference and Exhibition*, March 19-23, 2023.
8. Texas Instruments [Power-supply filter ICs](#) landing page.
9. [TPSF12C1](#) and [TPSF12C1-Q1](#) common-mode active EMI filters for single-phase systems.
10. [TPSF12C3](#) and [TPSF12C3-Q1](#) common-mode active EMI filters for three-phase systems.
11. Texas Instruments technical article: [How a stand-alone active EMI filter IC shrinks common-mode filter size](#)

IMPORTANT NOTICE AND DISCLAIMER

TI PROVIDES TECHNICAL AND RELIABILITY DATA (INCLUDING DATA SHEETS), DESIGN RESOURCES (INCLUDING REFERENCE DESIGNS), APPLICATION OR OTHER DESIGN ADVICE, WEB TOOLS, SAFETY INFORMATION, AND OTHER RESOURCES "AS IS" AND WITH ALL FAULTS, AND DISCLAIMS ALL WARRANTIES, EXPRESS AND IMPLIED, INCLUDING WITHOUT LIMITATION ANY IMPLIED WARRANTIES OF MERCHANTABILITY, FITNESS FOR A PARTICULAR PURPOSE OR NON-INFRINGEMENT OF THIRD PARTY INTELLECTUAL PROPERTY RIGHTS.

These resources are intended for skilled developers designing with TI products. You are solely responsible for (1) selecting the appropriate TI products for your application, (2) designing, validating and testing your application, and (3) ensuring your application meets applicable standards, and any other safety, security, regulatory or other requirements.

These resources are subject to change without notice. TI grants you permission to use these resources only for development of an application that uses the TI products described in the resource. Other reproduction and display of these resources is prohibited. No license is granted to any other TI intellectual property right or to any third party intellectual property right. TI disclaims responsibility for, and you will fully indemnify TI and its representatives against, any claims, damages, costs, losses, and liabilities arising out of your use of these resources.

TI's products are provided subject to [TI's Terms of Sale](#) or other applicable terms available either on [ti.com](https://www.ti.com) or provided in conjunction with such TI products. TI's provision of these resources does not expand or otherwise alter TI's applicable warranties or warranty disclaimers for TI products.

TI objects to and rejects any additional or different terms you may have proposed.

Mailing Address: Texas Instruments, Post Office Box 655303, Dallas, Texas 75265
Copyright © 2023, Texas Instruments Incorporated